C.P. No. 412
(20,499)
A.R.C. Technical Report

C.P. No. 412
(20,499)
A.R.C. Technical Report

MINISTRY OF SUPPLY

AERONAUTICAL RESEARCH COUNCIL

CURRENT PAPERS

Theoretical Analysis of the Heating of a Composite Slab, with applications to the Kinetic Heating of an Aircraft Wing

by

E. C. Capey, B.Sc. & K. I. McKenzie, Ph.D.

LONDON: HER MAJESTY'S STATIONERY OFFICE

1958

PRICE 4s. 6d. NET

C.P. No.412

U.D.C. No. 629.13.014.3 : 533.6.011.6 : 536.212.2 : 621-419.4

Technical Note No. Structures 243

June, 1958

ROYAL AIRCRAFT ESTABLISHMENT

THEORETICAL ANALYSIS OF THE HEATING OF A COMPOSITE SLAB, WITH APPLICATIONS TO THE KINETIC HEATING OF AN AIRCRAFT WING

by

E. C. Capey, B.Sc.

and

K. I. McKenzie, Ph.D.

SUMMARY

The transient temperature distribution is derived for a composite slab, heated by raising the air temperature on one side at a constant rate to a maximum. Numerical results are evaluated on a digital computer from the theoretical solution, which is obtained in series form. Results are obtained for the temperature difference across the skin in an aircraft wing covered by insulative material; these results show that the effect of the insulative material could be calculated with sufficient accuracy by neglecting its heat capacity. The computer programmes are applicable to any problem in which there is no heat transfer at the cold surface.

LIST OF CONTENTS

LIST OF APPENDICES

LIST OF TABLES

LIST OF ILLUSTRATIONS

1 LIST OF SYMBOLS

ℓ = thickness of lower section of slab

ℓ' = thickness of upper section of slab

k = thermal conductivity of lower section of slab

k' = thermal conductivity of upper section of slab

ρ = density of lower section of slab

ρ' = density of upper section of slab

c = specific heat of lower section of slab

c' = specific heat of upper section of slab

$K = \frac{k}{\rho c}$ = diffusivity of lower section of slab

$K' = \frac{k'}{\rho' c'}$ = diffusivity of upper section of slab

h = heat transfer coefficient on lower surface

h' = heat transfer coefficient on upper surface

x = distance from lower surface of slab

t = time

$\phi(t)$ = adiabatic wall temperature on lower surface

$\phi'(t)$ = adiabatic wall temperature on upper surface

$V(x,t)$ = temperature in lower section of slab

$V'(x,t)$ = temperature in upper section of slab

T = time taken to reach final temperature

β = final temperature

p = Laplace transform for the time

ε = $\ell i \sqrt{p/K}$

$\overline{\phi}'(p)$ = Laplace transform of $\phi'(t)$

$\overline{V}, \overline{V}'$ = Laplace transforms of V, V'

A, B, C, D = functions of p in equations (22) and (23)

$\alpha = \frac{k}{k'}\sqrt{\frac{K'}{K}}$

$\gamma = \frac{\ell'}{\ell}\sqrt{\frac{K}{K'}}$

$\lambda = \frac{h\ell}{k}$

} non-dimensional constants

$\mu = \frac{k'}{h'\ell}\sqrt{\frac{K}{K'}}$

$\Lambda = \frac{\ell/k}{\ell'/k' + 1/h'}$

} non-dimensional constants

$F(\varepsilon)$ = expression given in equation (11)

a_n = constants given by equation (12)

b_n = coefficients in expansion of $\overline{V}$ in equation (34)

$N(\varepsilon)$ = numerator in expression in equation (28) or (29)

2 INTRODUCTION

If the external surfaces of any of the wings shown in Fig.1 are heated, while the internal surfaces remain cold, thermal stresses are produced in the plating. An estimate of the thermal stress can be obtained by treating the wing as a slab, one side of which is heated, while the other side is subjected to boundary conditions depending on the type of wing.

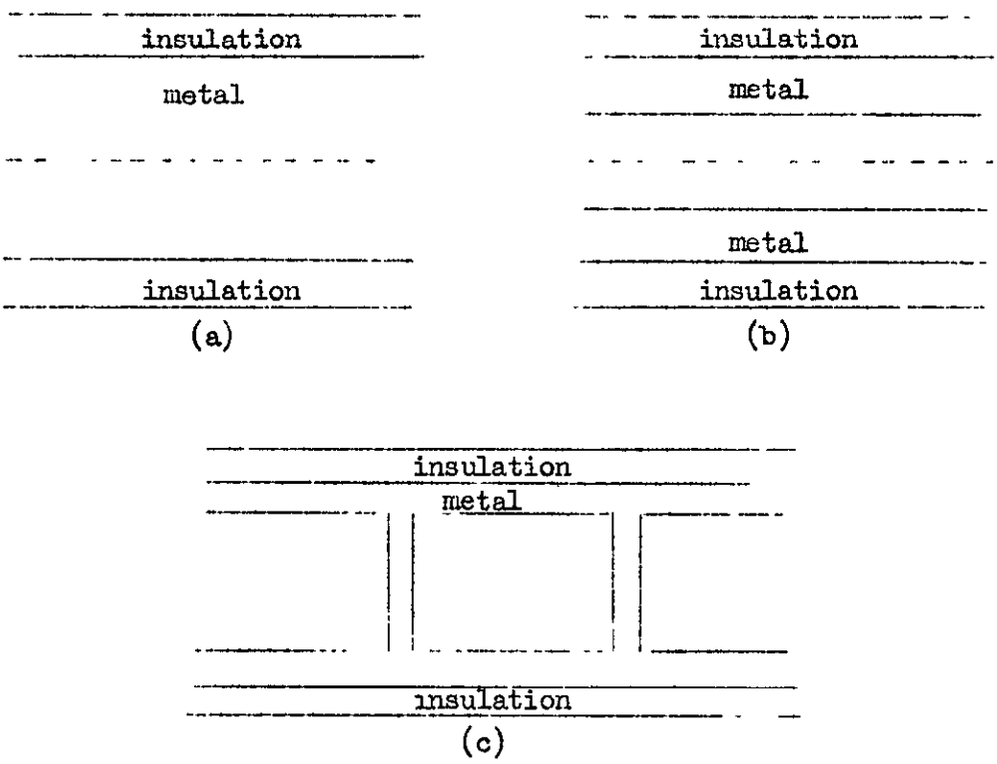

Fig.1. Aircraft wings subject to surface heating.

The problem reduces to that of finding the temperature distribution in a composite slab, of the type shown in Fig.2, where ϕ and ϕ' are the adiabatic wall temperatures on either side of the slab, and h and h' are the heat transfer coefficients between the air and the metal and between the air and the insulation respectively.

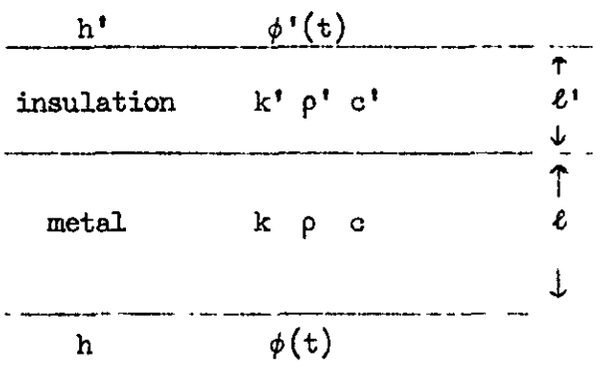

Fig.2 Composite slab showing notation.

All the relevant equations are linear in the temperature, thus allowing solutions to be obtained by superposition. The case here considered is that of an aircraft which is accelerated in such a manner that the adiabatic wall temperature ϕ' rises linearly from an initial value, taken to be zero, to a final value β, as shown in Fig.3(a). This solution can be obtained by the superposition of an infinite series of solutions for a step function variation of ϕ', as shown in Fig.3(b).

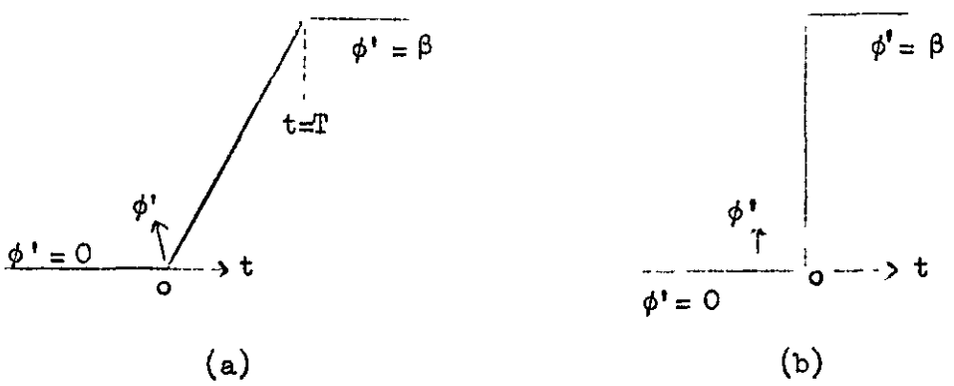

Fig.3. Variation of adiabatic wall temperature with time.

The analysis of the slab shown in Fig.2 applies directly to the wing in Fig.1(b). It also applies to the skin of the wing in Fig.1(c) except near to the webs, and to the wing in Fig.1(a) if h is put equal to zero, since, from symmetry, no heat crosses the line A'B'C'D'.

The temperature distribution and thermal stresses in a slab of the type shown in Fig.2 have been calculated by Parkes[1], making the assumptions that the heat capacity of the insulative material can be neglected and that no heat leaves the lower surface of the metal, which is equivalent to putting h equal to zero. In this report the temperature distribution and thermal stresses are obtained for the general case, when the heat capacity of the insulation is taken into account, and when h may have any value.

The maximum temperature difference across the metal part of the slab is taken as a measure of the thermal stress. This maximum temperature difference and the time at which it occurs are computed for various materials, thicknesses and heat transfer coefficients using a digital computer. A comparison is made between the results obtained by Parkes neglecting the heat capacity of the insulative material and the more accurate results obtained from the analysis in this paper.

3 METHOD OF SOLUTION

In order to obtain the temperature distribution in the slab shown in Fig.2, it is necessary to obtain a solution of the differential equation

$$\frac{\partial^2 V}{\partial x^2} - \frac{1}{K} \cdot \frac{\partial V}{\partial t} = 0 \qquad (1)$$

in the lower section of the slab, where K is the diffusivity of the metal, given by the equation

$$K = \frac{k}{\rho c} , \qquad (2)$$

and of the differential equation

$$\frac{\partial^2 V'}{\partial x^2} - \frac{1}{K'} \cdot \frac{\partial V'}{\partial t'} = 0 \qquad (3)$$

in the upper section, where

$$K' = \frac{k'}{\rho' c'} . \qquad (4)$$

It is assumed that k and ρc are constant over the range of temperatures involved.

The temperature and heat flow must be continuous over the boundary between the two materials, so that

$$V(\ell) = V'(\ell) \qquad (5)$$

and

$$k \left(\frac{\partial V}{\partial x}\right)_{\ell} = k' \left(\frac{\partial V'}{\partial x}\right)_{\ell'} . \qquad (6)$$

The boundary condition at the lower edge, x = 0, is that the heat flow is equal to the heat transfer coefficient times the difference between the adiabatic wall temperature and the surface temperature, that is

$$k \left(\frac{\partial V}{\partial x}\right)_{o} - h \left\{ V(o) - \phi(t) \right\} = 0 , \qquad (7)$$

while at the upper edge, at $x = \ell + \ell'$, the condition is that

$$k' \left(\frac{\partial V'}{\partial x}\right)_{\ell+\ell'} + h' \left\{ V(\ell+\ell') - \phi'(t) \right\} = 0 . \qquad (8)$$

The initial condition is that

$$V = V' = 0 \qquad (9)$$

at

$$t = 0.$$

The solution is to be obtained for the variation of ϕ' shown in Fig.3(b) with $\phi = 0$ throughout.

A Laplace transformation is carried out on equations (1) to (9) in Appendix 1, and the inverse transformation gives the solution

$$V(x,t) = \beta\left\{ \frac{\frac{1}{h}+\frac{x}{k}}{\frac{1}{h}+\frac{\ell}{k}+\frac{\ell'}{k'}+\frac{1}{h'}} + \sum_n a_n\left(\cos \varepsilon_n \frac{x}{\ell}+\frac{h\ell}{k\varepsilon_n} \sin \varepsilon_n \frac{x}{\ell}\right) \exp(-K\varepsilon_n^2 t/\ell^2) \right\} \qquad (10)$$

where the first term represents the steady state solution, and the second term the transient solution. The summation in the transient term is taken over the values of ε_n corresponding to the solutions of the equation

$$F(\varepsilon) = \left\{(\cos \varepsilon \cos \gamma\varepsilon - \alpha \sin \varepsilon \sin \gamma\varepsilon) - \varepsilon\mu\ (\cos \varepsilon \sin \gamma\varepsilon + \alpha \sin \varepsilon \cos \gamma\varepsilon)\right\}$$

$$+ \frac{\lambda}{\varepsilon}\left\{(\sin \varepsilon \cos \gamma\varepsilon + \alpha \cos \varepsilon \sin \gamma\varepsilon\right.$$

$$\left. - \varepsilon\mu\ (\sin \varepsilon \sin \gamma\varepsilon - \alpha \cos \varepsilon \cos \gamma\varepsilon) \right\} = 0, \qquad (11)$$

where α, γ and μ are non-dimensional parameters which depend on the properties of the materials and the heat transfer coefficients. The coefficients a_n are given by the equation

$$a_n = \frac{2}{\varepsilon_n\left(\frac{dF}{d\varepsilon}\right)_{\varepsilon_n}} . \qquad (12)$$

There are an infinite number of terms in the series for the transient temperature distribution; but as n increases a_n diminishes rapidly, so that only the first few terms in the series need to be evaluated.

In order to obtain the temperature distribution when the adiabatic wall temperature varies as in Fig.3(a), solutions of the form shown in equation (10) are superposed and integrated. Expressions for the temperature distribution before and after the maximum adiabatic wall temperature is reached are given in Appendix 1.

The temperature difference, $V(\ell) - V(o)$, across the metal section is a rough measure of the thermal stress. When there is no heat transfer across the lower edge of the slab, that is $h = 0$, $V(\ell) - V(o)$ is given by the equations

$$V(\ell) - V(o) = \beta \sum_n a_n (\cos \varepsilon_n - 1) \frac{\{1 - \exp(-K\varepsilon_n^2 t/\ell^2)\}}{K\varepsilon_n^2 t/\ell^2} \qquad (t < T) \quad (13)$$

and

$$V(\ell) - V(o) = \beta \sum_n a_n (\cos \varepsilon_n - 1) \frac{\{\exp(K\varepsilon_n^2 T/\ell^2) - 1\} \exp(-K\varepsilon_n^2 t/\ell^2)}{K\varepsilon_n^2 T/\ell^2} \qquad (14)$$

$(t > T)$.

A computation for evaluating and maximising the second of these expressions was programmed for the DEUCE digital computer. It was not necessary to evaluate the former expression, since the maximum never lies in that range. Results for the maximum value of $V(\ell) - V(o)$ and for the time at which this maximum occurs were obtained for a number of different materials, thicknesses and heat transfer coefficients, and are given in Tables 2 and 3.

Another case which might be of some interest is that of the slab with an infinite heat transfer coefficient h on the lower surface. This might be approximately realised by the use of a liquid to cool the lower surface. The maximum temperature difference in this case is simply the steady state temperature difference

$$V(\ell) - V(o) = \frac{\frac{\ell}{k}}{\frac{\ell}{k} + \frac{\ell'}{k'} + \frac{1}{h'}} \beta \, . \qquad (15)$$

4 APPROXIMATE METHOD

Parkes[1] obtained an approximate solution to the problem of the composite slab by assuming that, although the heat resistance of the insulative material is greater than or comparable with that of the metal, its heat capacity is negligible. Parkes' solution follows simply from the general analysis, and is obtained in Appendix 2. It is shown that, in the case when h vanishes and ϕ is taken to be a step function,

$$V(x,t) = \beta \left\{ 1 + \sum_n a_n \cos\left(\varepsilon_n \frac{x}{\ell}\right) \exp(-K\varepsilon_n^2 t/\ell^2) \right\} , \qquad (16)$$

where

$$\varepsilon_n \tan \varepsilon_n = \frac{1}{\alpha(\gamma + \mu)} = \Lambda \, , \qquad (17)$$

$$= \frac{\ell/k}{\ell'/k' + 1/h'}$$

and

$$a_n = \frac{-2\Lambda \sec \varepsilon_n}{\Lambda + \Lambda^2 + \varepsilon_n^2} \qquad (18)$$

5 THE PROGRAMME FOR DEUCE

The programme for this computation is in two separate parts. The first part computes the ε_n's and a_n's from equations (11) and (12) using a subroutine to evaluate $F(\varepsilon)$ and $\frac{dF}{d\varepsilon}$ for any ε. The second part uses these values and a subroutine to evaluate $V(\ell) - V(o)$ at any time, to find the maximum of $V(\ell) - V(o)$ and the time at which it occurs. A schematic representation of the programme is given in Appendix 3.

6 DISCUSSION OF RESULTS

It is shown in Appendix 1 that the solution to the general problem depends on five non-dimensional variables, α, γ, μ, λ and $\frac{KT}{\ell^2}$. All the calculations were made assuming $\lambda = 0$, that is, no heat flow over the lower surface of the metal.

The thermal properties of aluminium alloy, stainless steel, titanium, Durestos and paint are shown in Table 1. Since, as far as those properties are concerned, titanium is similar to stainless steel, and paint to Durestos, it was decided that only two cases needed to be considered:

(i) Durestos on aluminium alloy and

(ii) Durestos on stainless steel.

Table 2 shows the values of α, γ and μ corresponding to various thicknesses of metal plate, thicknesses of insulation and heat transfer coefficients. It was considered impractical to have a metal plate more than 2 in. thick, or a heat transfer coefficient greater than 0.1 joules/cm^2 sec ^oO (175 Btu/ft^2 hr ^oF). Computations were carried out for all other cases where the thermal stresses would be appreciable. Altogether, 28 computations were carried out, 17 with $\gamma \neq 0$ and 11 with $\gamma = 0$; and in each case $\frac{KT}{\ell^2}$ was given the values 0, 2.5 and 5. $\frac{KT}{\ell^2} = 5$ corresponds to a very slow acceleration, so that the solutions for most practical cases can be obtained by interpolation between the values for $\frac{KT}{\ell^2} = 0$, 2.5 and 5.

Putting $\gamma = 0$ is equivalent to neglecting the heat capacity of the insulation, and in this case the temperature distribution for any particular value of $\frac{KT}{\ell^2}$ depends only on $\Lambda = \frac{1}{\alpha(\gamma+\mu)}$. Fig.4 shows values of $(V_\ell - V_o)/\beta$ plotted against Λ for $\frac{KT}{\ell^2} = 0$, 2.5 and 5. The results for $\gamma = 0$ are shown as continuous graphs and those for $\gamma \neq 0$ as small circles. It can be seen that the small circles lie very near to the continuous lines. Thus, in all practical cases, it is permissible to assume that $\gamma = 0$ and use the graphs of Fig.4. When the solutions with $\gamma = 0$ and $\gamma \neq 0$ were compared more closely, it was found that with $\gamma \neq 0$ the maximum temperature difference is a little lower and takes rather longer to reach than with $\gamma = 0$, for the same values of Λ and $\frac{KT}{\ell^2}$. Results for $(V_\ell - V_o)_{max}/\beta$ and t_{max} are shown in Table 3 with $\frac{KT}{\ell^2} = 0$, 2.5 and 5 for the 28 sets of values of α, γ and μ.

The actual temperature distribution was worked out for a sample case. Graphs of V against t are given in Fig.5 at 7 points in the metal and insulation, for T = 0 (that is, for instantaneous acceleration), $\Lambda = 1$, $\gamma = 0.267$, $\alpha = 2.5$ and $\mu = 0.133$. Beside these graphs small circles are drawn to represent the temperature which would be reached at the same place at the same time if T = 0, $\Lambda = 1$, $\gamma = 0$ and $\mu = 0.133$. This figure illustrates the fact that when $\gamma \neq 0$ the heat capacity of the insulation slows down the passage of heat into the slab, so that it takes longer for the slab to reach any given temperature.

7 CONCLUSIONS

The temperature distribution in a composite slab consisting of a layer of thermally insulative material fixed to a metal plate, is worked out by an analytical method for the case where the temperature of the air adjacent to the insulation increases linearly from an initial to a final value. It is assumed that the heat transfer coefficients on both faces of the slab remain constant as the air temperature increases. This problem can be taken to represent the kinetic heating of an aircraft wing.

An approximate analysis of the problem of a wing covered with insulative material is due to Parkes[1], who uses the simplifying assumption that, while the thermal resistance of the insulative material is comparable with or greater than that of the metal, its heat capacity is sufficiently small to be negligible.

The most practical case is that in which there is no heat flow over the air-metal surface; and all the computations are done using this condition. The maximum temperature difference across the metal plate, which is a rough measure of the thermal stress, is calculated numerically for all combinations of materials, thicknesses, and heat transfer coefficients thought likely to be of practical interest. The computations show that the thermal stresses will be small unless the skin thickness exceeds 1" for an aluminium skin, or $\frac{1}{4}$" for a stainless steel skin, and, where they do occur, they can be reduced considerably by a thin layer of insulation such as Durestos or paint. These results were compared with those obtained using Parkes' simplified theory, and it was found that, while the exact theory gives a slightly smaller value of the maximum temperature difference across the metal plate, and also retards the occurrence of this maximum a little, both of these effects are so small as to make the use of the simplified theory fully justified.

A table of results is presented showing the maximum temperature difference and the time taken to reach it for all the cases computed. A graph is drawn showing this maximum temperature difference, and comparing the exact with the simplified theory; and, for a sample case, a series of graphs is drawn showing the way in which the temperature changes with time at various points in the metal and insulation.

The apportionment of authorship is: analysis by E. C. Capey; computation by K. I. McKenzie.

LIST OF REFERENCES

Ref.No.	Author	Title, etc.
1	Parkes, E.W.	The alleviation of thermal stresses. Aircraft Engineering, Vol.25, pp.51-53, February, 1953.

APPENDIX 1

SOLUTION OF THE HEAT FLOW EQUATIONS FOR A COMPOSITE SLAB

The temperature distribution across the slab is obtained by taking the Laplace transform of the heat flow equations, substituting the boundary conditions, and then carrying out the inverse transformation.

The Laplace transforms of equations (1) and (3) are

$$\left.\begin{aligned}\left(\frac{\partial^2}{\partial x^2} - \frac{p}{K}\right)\bar{V}(x,p) &= -\frac{1}{K}V(x,o)\\ \text{and}\qquad \left(\frac{\partial^2}{\partial x^2} - \frac{p}{K'}\right)\bar{V}'(x,p) &= -\frac{1}{K'}V'(x,o)\ .\end{aligned}\right\} \tag{19}$$

Substituting

$$\varepsilon = \ell i\sqrt{p/K}\ , \tag{20}$$

and using equation (9) to eliminate the right hand sides, equations (19) give

$$\left.\begin{aligned}\left(\frac{\partial^2}{\partial x^2} + \frac{\varepsilon^2}{\ell^2}\right)\bar{V}(x,p) &= 0\\ \text{and}\qquad \left(\frac{\partial^2}{\partial x^2} + \frac{K}{K'}\cdot\frac{\varepsilon^2}{\ell^2}\right)\bar{V}(x,p) &= 0\ ,\end{aligned}\right\} \tag{21}$$

the general solutions of which are

$$\bar{V}(x,p) = A(p)\cos\frac{\varepsilon x}{\ell} + B(p)\sin\frac{\varepsilon x}{\ell} \tag{22}$$

$$\bar{V}'(x,p) = C(p)\cos\varepsilon\sqrt{\frac{K}{K'}}\cdot\frac{x}{\ell} + D(p)\sin\varepsilon\sqrt{\frac{K}{K'}}\cdot\frac{x}{\ell}\ , \tag{23}$$

where A, B, C and D are functions of p.

On applying the Laplace transformation to equations (5) to (8), they become:-

$$\bar{V}(\ell) = \bar{V}'(\ell), \tag{24}$$

$$k\left(\frac{\partial\bar{V}}{\partial x}\right)_\ell = k'\left(\frac{\partial\bar{V}'}{\partial x}\right)_\ell\ , \tag{25}$$

$$k\left(\frac{\partial \bar{V}}{\partial x}\right)_o - h\,\bar{V}(o) = 0 \qquad (26)$$

and

$$k'\left(\frac{\partial V'}{\partial x}\right)_{\ell+\ell'} + h'\left\{\bar{V}(\ell+\ell') - \frac{\beta}{p}\right\} = 0 \qquad (27)$$

where $\phi(t)$ is taken to be zero, and $\phi'(t)$ a step function as shown in Fig.3(b).

On combining these with equations (22) and (23), A, B, C and D are evaluated, giving

$$\bar{V}(x,p) = \beta\left(\cos \varepsilon x/\ell + \frac{\lambda}{\varepsilon}\sin \varepsilon x/\ell\right)\Big/ p\,F(\varepsilon) \qquad (28)$$

$$V'(x,p) = \beta\left[\left(\cos\varepsilon + \frac{\lambda}{\varepsilon}\sin\varepsilon\right)\cos\left\{\varepsilon\sqrt{\frac{K}{K'}}\left(\frac{x}{\ell}\right) - 1\right)\right\}$$

$$- \alpha\left(\sin\varepsilon - \frac{\lambda}{\varepsilon}\cos\varepsilon\right)\sin\left\{\varepsilon\sqrt{\frac{K}{K'}}\left(\frac{x}{\ell} - 1\right)\right\}\Big/ pF(\varepsilon) \qquad (29)$$

where

$$F(\varepsilon) = \left\{(\cos\varepsilon\cos\gamma\varepsilon - \alpha\sin\varepsilon\sin\gamma\varepsilon) - \varepsilon\mu(\cos\varepsilon\sin\gamma\varepsilon + \alpha\sin\varepsilon\cos\gamma\varepsilon)\right\}$$

$$+ \frac{\lambda}{\varepsilon}\left\{(\sin\varepsilon\cos\gamma\varepsilon + \alpha\cos\varepsilon\sin\gamma\varepsilon - \varepsilon\mu(\sin\varepsilon\sin\gamma\varepsilon - \alpha\cos\varepsilon\cos\gamma\varepsilon)\right\} \qquad (30)$$

and

$$\alpha = \frac{k}{k'}\sqrt{\frac{K'}{K}}$$

$$\gamma = \frac{\ell'}{\ell}\sqrt{\frac{K}{K'}}$$

$$\mu = \frac{k'}{h'\ell}\sqrt{\frac{K}{K'}}$$

and

$$\lambda = \frac{h\ell}{k}.$$

Expressions for $V(x,t)$ and $V'(x,t)$ can be obtained by separating the expressions in equation (28) and (29) into partial fractions, then carrying out the inverse Laplace transformation on the separate fractions. As

$$\varepsilon = \ell i\sqrt{p/K}$$

both the numerators and denominators in equations (28) and (29) are converging power series in p, and can therefore be represented to any degree of accuracy by polynomials to the $(M-1)^{th}$ and $(M+1)^{th}$ powers respectively; and consequently $\overline{V}(x,p)$ can be broken up into partial fractions as follows:

$$\overline{V}(x,p) = \frac{b_o}{p} + \frac{b_1}{p-p_1} + \frac{b_2}{p-p_2} \cdots \frac{b_M}{p-p_M} \tag{31}$$

where, if M is large, the p_n's approximate to the roots of equation (30), provided that this equation does not possess multiple roots. If equation (30) had possessed multiple roots for any of the sets of values of γ, α and μ used in the computations, this would have been noticed; but in fact it did not occur.

If both sides of equation (31) are multiplied by $(p-p_n)$, and then p tends to p_n, b_n can be evaluated and is given by the equation

$$\begin{aligned} b_n &= \lim_{p \to p_n} \overline{V}(x,p)(p-p_n) \\ &= \frac{N(p_n)}{p_n \left(\frac{dF}{dp}\right)_{p_n}} \\ &= \frac{2N(\varepsilon_n)}{\varepsilon_n \left(\frac{dF}{d\varepsilon}\right)_{\varepsilon_n}}, \end{aligned} \tag{32}$$

while

$$b_o = \frac{N(o)}{F(o)}, \tag{33}$$

where N is the numerator of the expression in equation (28) or (29).

The inverse transformation of equation (31) is

$$V(x,t) = b_o + \sum_{n=1}^{\infty} b_n e^{p_n t}. \tag{34}$$

On substituting equations (32) and (33) into equation (34), then substituting into the constant term b_o for α, γ, μ and λ, the temperature distribution is given by the equations

$$V(x,t) = \beta \left\{ \frac{\frac{1}{h}+\frac{x}{k}}{\frac{1}{h}+\frac{\ell}{k}+\frac{\ell'}{k'}+\frac{1}{h'}} + \sum_n a_n \left(\cos \varepsilon_n \frac{x}{\ell} + \frac{\lambda}{\varepsilon_n} \sin \varepsilon_n \frac{x}{\ell} \right) \exp(-K\varepsilon_n^2 t/\ell^2) \right\} \tag{35}$$

and

$$V'(x,t) = \beta\left\{\frac{\frac{1}{h}+\frac{\ell}{k}+\frac{x-\ell}{k'}}{\frac{1}{h}+\frac{\ell}{k}+\frac{\ell'}{k'}+\frac{1}{h'}} + \sum_n a_n\left[\left(\cos\varepsilon_n+\frac{\lambda}{\varepsilon_n}\sin\varepsilon_n\right)\cos\left\{\varepsilon_n\sqrt{\frac{K}{K'}}\left(\frac{x}{\ell}-1\right)\right\}\right.\right.$$

$$\left.\left. - \alpha\left(\sin\varepsilon_n-\frac{\lambda}{\varepsilon_n}\cos\varepsilon_n\right)\sin\left\{\varepsilon_n\sqrt{\frac{K}{K'}}\left(\frac{x}{\ell}-1\right)\right\}\right]\exp(-K\varepsilon_n^2\, t/\ell^2)\right\}, \quad (36)$$

where the ε_n's are the solutions of the equation

$$F(\varepsilon_n) = 0 ,$$

and the a_n's are given by the equation

$$a_n = 2/\varepsilon_n\left(\frac{dF}{d\varepsilon}\right)_{\varepsilon_n} \quad (37)$$

Equations (35) and (36) give the temperature distribution resulting from an applied air temperature as shown in Fig.3(b). If this distribution is called $\phi_1'(t)$, then the distribution in Fig.3(a) can be written as

$$\left.\begin{aligned} \phi' &= \int_o^t \frac{1}{T}\phi_1'(z)\,dz \quad \text{for } t < T \\ \text{or} \\ \phi' &= \int_o^T \frac{1}{T}\phi_1'(z)\,dz \quad \text{for } t > T . \end{aligned}\right\} \quad (38)$$

As all the equations are linear the solution for this case can be obtained by superposition, and $V(x,t)$ is given by the equation

$$V(x,t) = \int_o^t \frac{\beta}{T}\left\{\frac{\frac{1}{h}+\frac{x}{k}}{\frac{1}{h}+\frac{\ell}{k}+\frac{\ell'}{k'}+\frac{1}{h'}} + \sum_n a_n\left(\cos\varepsilon_n\frac{x}{\ell}+\frac{\lambda}{\varepsilon_n}\sin\varepsilon_n\frac{x}{\ell}\right)\exp\{-K\varepsilon_n^2\,(t-z)/\ell^2\}\right\}dz$$

$$= \frac{\beta t}{T}\left(\frac{\frac{1}{h}+\frac{x}{k}}{\frac{1}{h}+\frac{\ell}{k}+\frac{\ell'}{k'}+\frac{1}{h'}}\right) + \beta\sum_n a_n\left(\cos\varepsilon_n\frac{x}{\ell}+\frac{\lambda}{\varepsilon_n}\sin\varepsilon_n\frac{x}{\ell}\right)\frac{\{1-\exp(-K\varepsilon_n^2\, t/\ell^2)\}}{KT\varepsilon_n^2/\ell^2}$$

$$\text{for } t < T \quad (39)$$

and

$$V(x,t) = \int_0^T \frac{\beta}{T}\left\{\frac{\frac{1}{h}+\frac{x}{k}}{\frac{1}{h}+\frac{\ell}{k}+\frac{\ell'}{k'}+\frac{1}{h'}} + \sum_n a_n\left(\cos\varepsilon_n\frac{x}{\ell}+\frac{\lambda}{\varepsilon_n}\sin\varepsilon_n\frac{x}{\ell}\right)\exp\{-K\varepsilon_n^2(t-z)/\ell^2\}\right\}dz$$

$$= \beta\left(\frac{\frac{1}{h}+\frac{x}{k}}{\frac{1}{h}+\frac{\ell}{k}+\frac{\ell'}{k'}+\frac{1}{h'}}\right)+\beta\sum_n a_n\left(\cos\varepsilon_n\frac{x}{\ell}+\frac{\lambda}{\varepsilon_n}\sin\varepsilon_n\frac{x}{\ell}\right)\frac{\{\exp(K\varepsilon_n^2 T/\ell^2)-1\}\exp(-K\varepsilon_n^2 t/\ell^2)}{KT\varepsilon_n{}^2/\ell^2}$$

for $t > T$. (40)

The temperature difference across the metallic section of the slab is $V(\ell) - V(o)$, which is given by the equations:-

$$\frac{V(\ell)-V(o)}{\beta} = \frac{\frac{\ell}{k}\cdot\frac{t}{T}}{\frac{1}{h}+\frac{\ell}{k}+\frac{\ell'}{k'}+\frac{1}{h'}} + \sum_n a_n\left(\cos\varepsilon_n+\frac{\lambda}{\varepsilon_n}\sin\varepsilon_n-1\right)\times\frac{\{1-\exp(-K\varepsilon_n^2\, t/\ell^2)\}}{KT\varepsilon_n{}^2/\ell^2} \quad \text{for } t < T \tag{41}$$

and

$$\frac{V(\ell)-V(o)}{\beta} = \frac{\frac{\ell}{k}}{\frac{1}{h}+\frac{\ell}{k}+\frac{\ell'}{k'}+\frac{1}{h'}} + \sum_n a_n\left(\cos\varepsilon_n+\frac{\lambda}{\varepsilon_n}\sin\varepsilon_n-1\right)\times\frac{\{\exp(K\varepsilon_n^2\, T/\ell^2)-1\}\exp(-K\varepsilon_n^2\, t/\ell^2)}{KT\varepsilon_n{}^2/\ell^2}$$

for $t > T$. (42)

Special cases

(i) No heat transfer on lower surface.

This is the case considered by Parkes, and is the one which is likely to be most practical. Equations for this case can be obtained by substituting $h = 0$ and $\lambda = 0$ into the equations derived above. The temperature difference across the metallic section of the slab is obtained from equations (41) and (42) and is

$$\frac{V(\ell)-V(o)}{\beta} = \sum_n a_n(\cos\varepsilon_n-1)\frac{\{1-\exp(-K\varepsilon_n^2\, t/\ell^2)\}}{KT\varepsilon_n{}^2/\ell^2} \quad \text{for } t < T \tag{43}$$

and

$$\frac{V(\ell) - V(o)}{\beta} = \sum_{n}' a_n (\cos \varepsilon_n - 1) \frac{\{\exp(K\varepsilon_n^2 T/\ell^2) - 1\} \exp(-K\varepsilon_n^2 t/\ell^2)}{KT\varepsilon_n^2/\ell^2} \quad \text{for } t > T . \tag{44}$$

The summation is carried out over those values of ε which obey the equation

$$F(\varepsilon) = (\cos \varepsilon \cos \gamma\varepsilon - \alpha \sin \varepsilon \sin \gamma\varepsilon) - \varepsilon\mu(\cos \varepsilon \sin \gamma\varepsilon + \alpha \sin \varepsilon \cos \gamma\varepsilon) = 0 . \tag{45}$$

The a_n's are given by equation (37), which can be expanded and becomes

$$a_n = \frac{-2/\varepsilon_n}{(1 + \alpha\gamma + \alpha\mu) \sin \varepsilon_n \cos \gamma\varepsilon_n - \varepsilon_n\mu(1 + \alpha\gamma) \sin \varepsilon_n \sin \gamma\varepsilon_n} + \tag{46}$$

$$+ \varepsilon_n\mu(\alpha + \gamma) \cos \varepsilon_n \cos \gamma\varepsilon_n + (\alpha + \gamma + \mu) \cos \varepsilon_n \sin \gamma\varepsilon_n$$

(ii) Perfect conduction on the lower surface.

Similar equations can be obtained for this case by letting h and λ tend to infinity. In this case the temperature difference always increases with time, so that the maximum temperature difference is the steady state temperature difference. This is obtained by making h, λ and t in equation (42) infinite, so that

$$\frac{V(\ell) - V(o)}{\beta} = \frac{\frac{\ell}{k}}{\frac{1}{h} + \frac{\ell}{k} + \frac{\ell'}{k'} + \frac{1}{h'}} . \tag{47}$$

APPENDIX 2

TEMPERATURE DISTRIBUTION WITH THE HEAT CAPACITY OF THE INSULATION NEGLECTED

When the thermal resistance $\frac{\ell'}{k'}$ of the insulative material is very much greater than the thermal resistance $\frac{\ell}{k}$ of the metal, the thermal stresses are negligible. On the other hand, when $\frac{\ell'}{k'}$ is very much less than $\frac{\ell}{k}$ the insulative material is ineffective. Therefore, analysis is required only for values of $\frac{\ell' k}{\ell k'}$ of the order of magnitude of 1. The insulation will naturally be a material with low conductivity, so that a considerable reduction in the thermal stresses will be obtained with a small thickness of insulation. Such a small thickness of insulation will have a small heat capacity, and this may be small enough to be negligible.

It follows from these assumptions that γ is small, and it is allowable to make the substitutions

$$\cos \gamma\varepsilon \rightarrow 1$$

and

$$\sin \gamma\varepsilon \rightarrow \gamma\varepsilon \ .$$

Substitution of these two relationships into equations (11) and (12) gives

$$F = \left(\cos \varepsilon_n - \frac{\lambda}{\varepsilon_n} \sin \varepsilon_n\right) - \frac{\varepsilon_n}{\Lambda}\left(\sin \varepsilon_n + \frac{\lambda}{\varepsilon_n} \cos \varepsilon_n\right) = 0 \qquad (48)$$

and

$$a_n = \frac{-2/\varepsilon_n}{\left(\sin \varepsilon_n + \frac{\lambda}{\varepsilon_n} \cos \varepsilon_n\right) + \frac{\varepsilon_n}{\Lambda}\left(\cos \varepsilon_n - \frac{\lambda}{\varepsilon_n} \sin \varepsilon_n\right) + \sin \varepsilon_n \left(\frac{1}{\Lambda} - \frac{\lambda}{\varepsilon_n^2}\right)} \ . \qquad (49)$$

The equations (35) and (39) to (44) which give the temperature in terms of the ε_n's and a_n's remain unchanged. For the special case when there is no heat transfer on the lower surface these equations reduce to

$$\varepsilon_n \tan \varepsilon_n = \Lambda \qquad (50)$$

and

$$a_n = -\frac{2\Lambda \sec \varepsilon_n}{\Lambda + \Lambda^2 + \varepsilon_n^2} \qquad (51)$$

These are the equations derived by Parkes. It is seen that in this case the temperature distribution in the metal does not depend on α, γ and μ separately, but only on Λ.

APPENDIX 3

SCHEMATIC REPRESENTATIONS OF THE DEUCE PROGRAMMES

1 Programme for evaluating ε_n and a_n

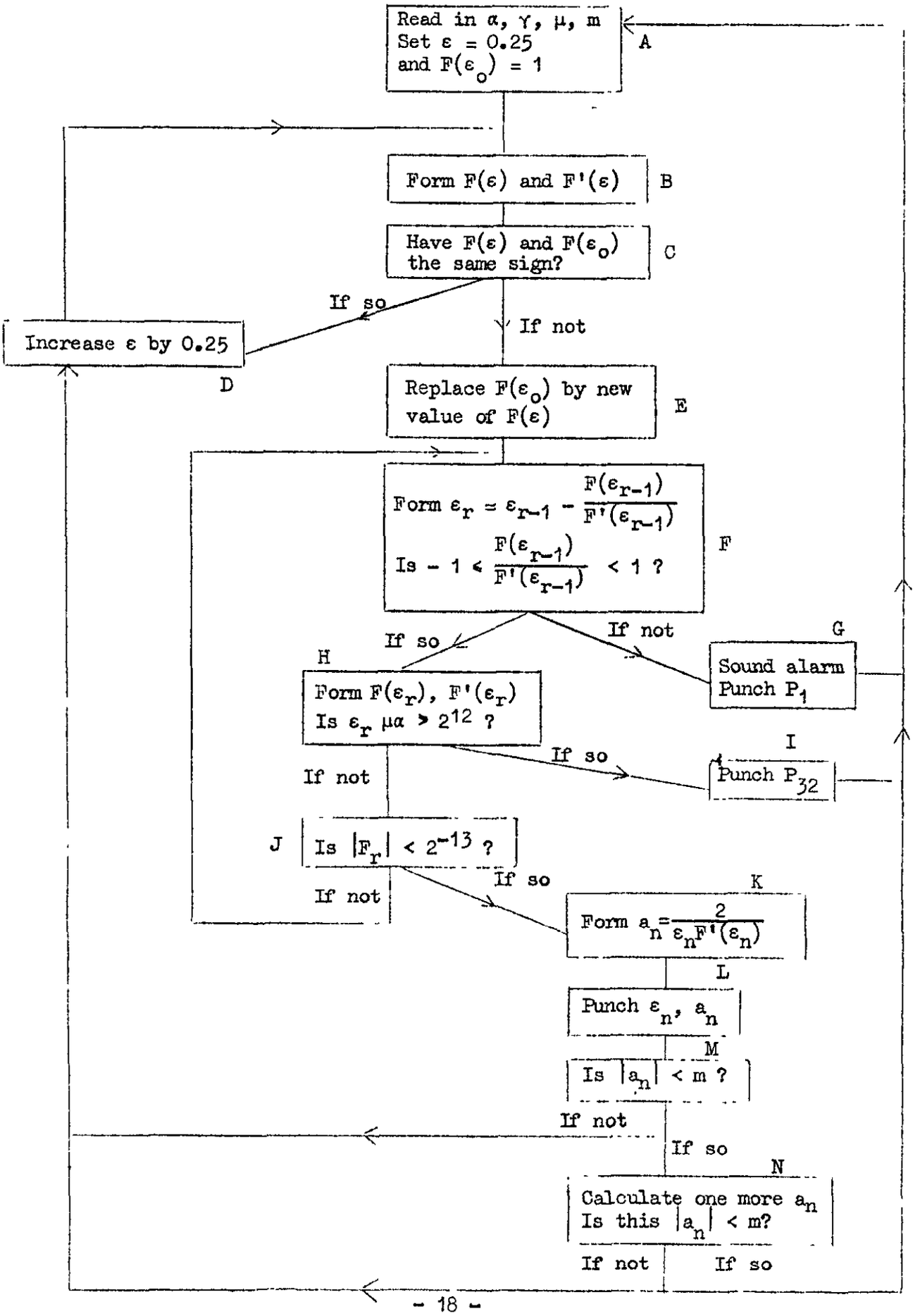

A The parameters are read in. α, γ and μ are given in the list of symbols, and m is the minimum value of a_n required. m was taken to be 2^{-6}.

B,C,D Starting from $\varepsilon = 0$, ε is increased by steps of 0.25 until $F(\varepsilon)$ changes sign. As soon as $F(\varepsilon)$ does change sign it is known that a root of $F(\varepsilon) = 0$ lies between this value of $F(\varepsilon)$ and the previous one.

E This value of $F(\varepsilon)$ becomes the new $F(\varepsilon_o)$, which will be used to find the next root.

F-J The root which has been approached is now evaluated, correct to twelve binary places, by the Newton-Raphson method. There is a limitation to the automatic divider on DEUCE, in that it fails if the quotient numerically exceeds 1. This is not likely in this case, and if it did occur, would mean that a root had been missed. If $\varepsilon_r \mu \alpha > 2^{12}$, the capacity of the machine would have been exceeded. In practice, neither of these things happened.

K To guard against the limitation of the divider in working out a_n, the divisor is tested to see if it is less than or equal to the dividend, and if so, is multiplied by 2. This is done repeatedly, until the quotient would be less than unity, and compensated for after division. In practice a_n never exceeded 2.

L ε_n, a_n are punched in binary to 20 places.

M,N a_n is tested to see whether it is less than m. If it is, one further a_n is computed to guard against the possibility of getting one small value of a_n between two larger ones.

Having worked out one set of ε_n's and a_n's, the programme returns to the beginning to read in more data.

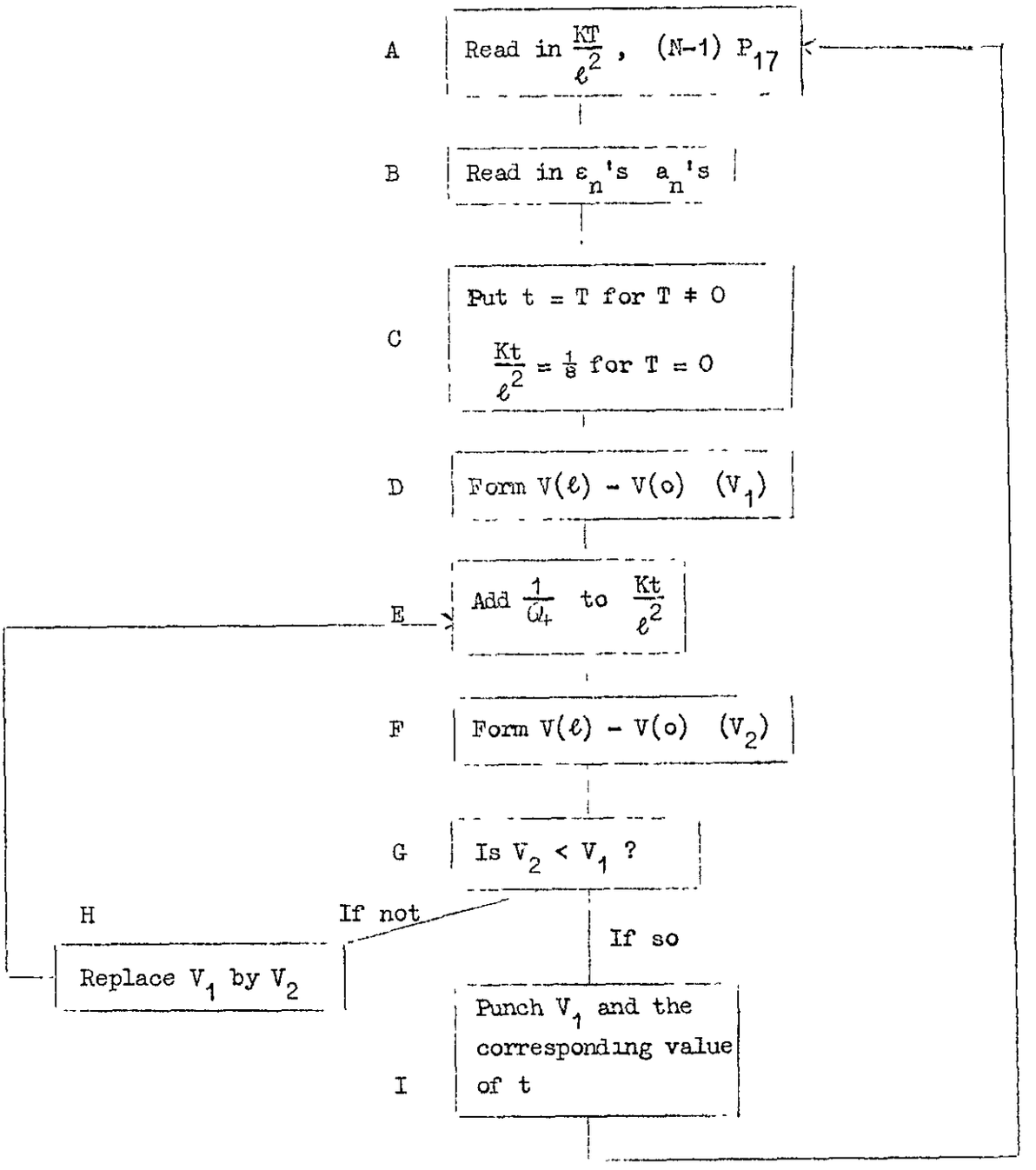
A
Read in $\frac{KT}{\ell^2}$, (N-1) P_{17}
B
Read in ε_n's a_n's
C
Put t = T for T ≠ 0
$\frac{Kt}{\ell^2} = \frac{1}{8}$ for T = 0
D
Form V(ℓ) - V(o) (V_1)
E
Add $\frac{1}{Q_4}$ to $\frac{Kt}{\ell^2}$
F
Form V(ℓ) - V(o) (V_2)
G
Is $V_2 < V_1$?
If not
If so
H
Replace V_1 by V_2
Punch V_1 and the corresponding value of t
I

A N is the number of terms taken in the series for $V(\ell) - V(o)$. In order not to exceed the capacity of the machine

$$\varepsilon^2 < \frac{2^9}{\frac{KT}{\ell^2} + 1}$$

which in turn sets a limitation on N.

B The ε_n's and a_n's must be stored for use in the subroutine for working out $V(\ell) - V(o)$.

C Owing to numerical inaccuracies it sometimes happens that for values of t near $t = 0$, $V(\ell) - V(o)$ decreases as t increases. This gives an apparent maximum at $t = 0$. To prevent this from appearing in the results, the first value of $\frac{Kt}{\ell^2}$ taken when $T = 0$ was $\frac{1}{8}$.

D–H $\frac{Kt}{\ell^2}$ is now repeatedly increased by $\frac{1}{64}$, working at $V(\ell) - V(o)$ each time, until a maximum of $V(\ell) - V(o)$ is reached.

I The value of $V(\ell) - V(o)$ nearest to the maximum, and the corresponding time, are punched to 22 binary places.

The programme returns to the beginning and reads in more data.

TABLE 1

Thermal Properties of Materials

	k (joules/cm sec ^{o}C)	c (joules/gm ^{o}C)	ρ (gm/cc)	K (in^2/sec)
Aluminium alloy	1.3	0.88	2.8	0.082
Stainless steel	0.2	0.50	7.8	0.0081
Titanium	0.15	0.61	4.5	0.0081
Durestos	0.004	1.3	1.7	0.00028
Paint	0.002 to 0.004	1.2	1.8	0.00015 to 0.0003

Case 1 Durestos (or paint) on aluminium alloy

$$\alpha = 20 \quad \gamma = 17\frac{\ell'}{\ell} \quad \mu = \frac{0.07}{h'\ell} .$$

Case 2 Durestos (or paint) on stainless steel (or titanium)

$$\alpha = 10 \quad \gamma = 5.5\frac{\ell'}{\ell} \quad \mu = \frac{0.022}{h'\ell} .$$

TABLE 2

Temperature Differences Across Selected Composite Slabs

Durestos on Aluminium Alloy

Thickness of metal ℓ (in)	Heat transfer coefficient h' (joules/cm^{2}sec$^\circ$C)	Thickness of insulation ℓ' (in)	Λ	α	γ	μ	Maximum Temperature Difference (T = 0) $(V_\ell - V_o)/\beta$	Computation number
> 2	Wing contains more than 4 inches of solid aluminium, which is impractical							
	> 0.1	Heat transfer coefficient more than 175 Btu/ft^{2}hr$^\circ$F, which is impractical						
2	0.1	0	0.357	20	0	0.14	0.143	Pa 4
	(175 Btu/ft^{2}hr$^\circ$F)	< 0.02	Effect of insulation is small					
		0.02	0.161	20	0.17	0.14	0.071	G 1
		0.04	0.104	20	0.34	0.14	0.048	G 2
		> 0.04	Thermal stresses negligible					
	0.05	0	0.178	20	0	0.28	0.078	Pa 2
		< 0.02	Effect of insulation small					
		0.02	0.111	20	0.17	0.28	0.051	G 3
		0.04	0.081	20	0.34	0.28	0.037	G 4
		> 0.04	Thermal stresses negligible					
	0.025	0	0.089	20	0	0.56	0.041	Pa 1
		Thermal stresses negligible, so no insulation required						
	< 0.025		Thermal stresses negligible					
1	0.1	0	0.178	20	0	0.28	0.078	Pa 2
		< 0.02	Effect of insulation is small					
		0.02	0.081	20	0.34	0.28	0.037	G 4
		> 0.02	Thermal stresses negligible					
	0.05	0	0.089	20	0	0.5	0.041	Pa 1
			Thermal stresses negligible					
0.5			Thermal stresses negligible					
Durestos on Stainless Steel								
2	0.1	0	2.27	10	0	0.044	0.491	See graph
		< 0.02	Effect of insulation is small					
		0.02	1.010	10	0.055	0.044	0.310	G 5
		0.04	0.649	10	0.11	0.044	0.227	G 6
		0.08	0.379	10	0.22	0.044	0.149	G 7

TABLE 2 (CONTD.)

Durestos on Stainless Steel (Contd.)

Thickness of metal ℓ (in)	Heat transfer coefficient h' (joules/cm^{2}sec$^\circ$C)	Thickness of insulation ℓ' (in)	Λ	α	γ	μ	Maximum Temperature Difference (T = 0) $(V_\ell - V_0)/\beta$	Computation number
2	0.1	0.16	0.207	10	0.44	0.044	~0.08	Similar to C 11
		0.32	0.108	10	0.88	0.044	~0.05	Similar to C 12
		> 0.32	Thermal stresses negligible					
	0.05	0	1.14	10	0	0.088	0.335	See graph
		< 0.02	Effect of insulation small					
		0.02	0.699	10	0.055	0.088	0.240	C 8
2	0.05	0.04	0.505	10	0.11	0.088	0.188	C 9
		0.08	0.325	10	0.22	0.088	0.151	C 10
		0.16	0.189	10	0.44	0.088	0.081	C 11
		0.32	0.103	10	0.88	0.088	0.046	C 12
		> 0.32	Thermal stresses negligible					
	0.025	0	0.568	10	0	0.176	0.206	Pa 5
		< 0.04	Effect of insulation small					
		0.04	0.350	10	0.11	0.176	0.140	C 13
		0.08	0.253	10	0.22	0.176	0.105	C 14
		0.16	0.162	10	0.44	0.176	0.071	C 15
		0.32	0.095	10	0.88	0.176	~0.05	Similar to C 12
		> 0.32	Thermal stresses negligible					
	0.0125	0	0.284	10	0	0.352	0.118	Pa 3
		< 0.08	Effect of insulation small					
		0.08	0.175	10	0.22	0.352	0.076	C 16
		0.16	0.126	10	0.44	0.352	0.056	C 17
		> 0.16	Thermal stresses negligible					
	0.00625	0	0.142	10	0	0.704	0.065	See graph
			No insulation needed. Thermal stresses negligible					
	< 0.00625		Thermal stresses negligible					
1	0.1	0	1.14	10	0	0.088	0.335	See graph
		< 0.01	Effect of insulation small					
		0.01	0.699	10	0.055	0.088	0.240	C 8
		0.02	0.505	10	0.11	0.088	0.188	C 9
		0.04	0.325	10	0.22	0.088	0.151	C 10

TABLE 2 (CONTD.)

Durestos on Stainless Steel (Contd.)

Thickness of metal ℓ (in)	Heat transfer coefficient h' (joules/cm^2-sec°C)	Thickness of insulation ℓ' (in)	Λ	α	γ	μ	Maximum Temperature Difference (T = 0) $(V_\ell - V_0)/\beta$	Computation number
		0.08	0.189	10	0.44	0.088	0.081	G 11
		0.16	0.103	10	0.88	0.088	0.046	G 12
	0.05	0	0.568	10	0	0.176	0.206	Pa 5
		0.02	0.350	10	0.11	0.176	0.140	G 13
		0.04	0.253	10	0.22	0.176	0.105	G 14
		0.08	0.162	10	0.44	0.176	0.071	G 15
		0.16	0.095	10	0.88	0.176	~ 0.05	Similar to G 12
	0.025	0	0.284	10	0	0.352	0.118	Pa 3
		0.04	0.175	10	0.22	0.352	0.076	G 16
		0.08	0.126	10	0.44	0.352	0.056	G 17
	0.0125	0	0.142	10	0	0.704	0.065	See graph
0.5	0.1	0	0.568	10	0	0.176	0.206	Pa 5
		0.01	0.350	10	0.11	0.176	0.140	G 13
		0.02	0.253	10	0.22	0.176	0.105	G 14
		0.04	0.162	10	0.44	0.176	0.071	G 15
		0.08	0.095	10	0.88	0.176	~0.05	Similar to G 12
	0.05	0	0.284	10	0	0.352	0.118	Pa 3
		0.02	0.175	10	0.22	0.352	0.076	G 16
		0.04	0.126	10	0.44	0.352	0.056	G 17
	0.025	0	0.142	10	0	0.704	0.065	See graph
0.25	0.1	0	0.284	10	0	0.352	0.118	Pa 3
		0.01	0.175	10	0.22	0.352	0.076	G 16
		0.02	0.126	10	0.44	0.352	0.056	G 17
	0.05	0	0.142	10	0	0.704	0.065	See graph
0.125	0.1	0	0.142	10	0	0.704	0.065	See graph
<0.125			Thermal stresses negligible					

TABLE 3

Computed Results

Comp. No.	Λ	γ	μ	α	$\frac{V(\ell)-V(o)}{\beta}$ for $\frac{KT}{\ell^2}=0$	$\frac{Kt_{max}}{\ell^2}$ for $\frac{KT}{\ell^2}=0$	$\frac{V(\ell)-V(o)}{\beta}$ for $\frac{KT}{\ell^2}=2.5$	$\frac{Kt_{max}}{\ell^2}$ for $\frac{KT}{\ell^2}=2.5$	$\frac{V(\ell)-V(o)}{\beta}$ for $\frac{KT}{\ell^2}=5$	$\frac{Kt_{max}}{\ell^2}$ for $\frac{KT}{\ell^2}=5$
G 1	0.161	0.17	0.14	20	0.0715	0.41	0.0623	2.61	0.0528	5.05
G 2	0.104	0.34	0.14	20	0.0477	0.48	0.0435	2.67	0.0390	5.11
G 3	0.111	0.17	0.28	20	0.0507	0.45	0.0461	2.64	0.0409	5.08
G 4	0.081	0.34	0.28	20	0.0374	0.52	0.0349	2.70	0.0319	5.14
G 5	1.010	0.055	0.044	10	0.3097	0.25	0.1672	2.50	0.0976	5.00
G 6	0.649	0.11	0.044	10	0.2272	0.27	0.1446	2.52	0.0927	5.00
G 7	0.379	0.22	0.044	10	0.1488	0.33	0.1110	2.55	0.0806	5.02
G 8	0.699	0.055	0.088	10	0.2401	0.27	0.1489	2.52	0.0938	5.00
G 9	0.505	0.11	0.088	10	0.1877	0.30	0.1294	2.53	0.0879	5.00
G 10	0.325	0.22	0.088	10	0.1309	0.34	0.1013	2.56	0.0760	5.02
G 11	0.189	0.44	0.088	10	0.0814	0.44	0.0696	2.64	0.0578	5.08
G 12	0.103	0.88	0.088	10	0.0458	0.70	0.0421	2.83	0.0379	5.25
G 13	0.350	0.11	0.176	10	0.1396	0.33	0.1061	2.55	0.0783	5.00
G 14	0.253	0.22	0.176	10	0.1055	0.37	0.0859	2.58	0.0678	5.03
G 15	0.162	0.44	0.176	10	0.0707	0.47	0.0618	2.66	0.0525	5.11
G 16	0.175	0.22	0.352	10	0.0761	0.42	0.0657	2.61	0.0552	5.06
G 17	0.126	0.44	0.352	10	0.0560	0.52	0.0503	2.70	0.0412	5.14
Pa 1	0.089	0	-	-	0.0415	0.45	0.0383	2.64	0.0348	5.08
Pa 2	0.178	0	-	-	0.0784	0.39	0.0674	2.58	0.0563	5.03
Pa 3	0.284	0	-	-	0.1180	0.34	0.0936	2.55	0.0741	5.02
Pa 4	0.357	0	-	-	0.1429	0.31	0.1078	2.53	0.0792	5.00
Pa 5	0.568	0	-	-	0.2064	0.28	0.1370	2.52	0.0904	5.00
Pa 6	0.9	0	-	-	0.2874	0.23	0.1622	2.50	0.0967	5.00
Pa 7	1.2	0	-	-	0.3464	0.22	0.1743	2.50	0.0986	5.00
Pa 8	1.5	0	-	-	0.3955	0.19	0.1815	2.50	0.0994	5.00
Pa 9	1.8	0	-	-	0.4374	0.19	0.1861	2.50	0.0997	5.00
Pa 10	2.1	0	-	-	0.4740	0.17	0.1892	2.50	0.0999	5.00
Pa 11	2.4	0	-	-	0.5053	0.16	0.1913	2.50	0.1001	5.00

WT.2078.C.P.412.K3 - Printed in Great Britain

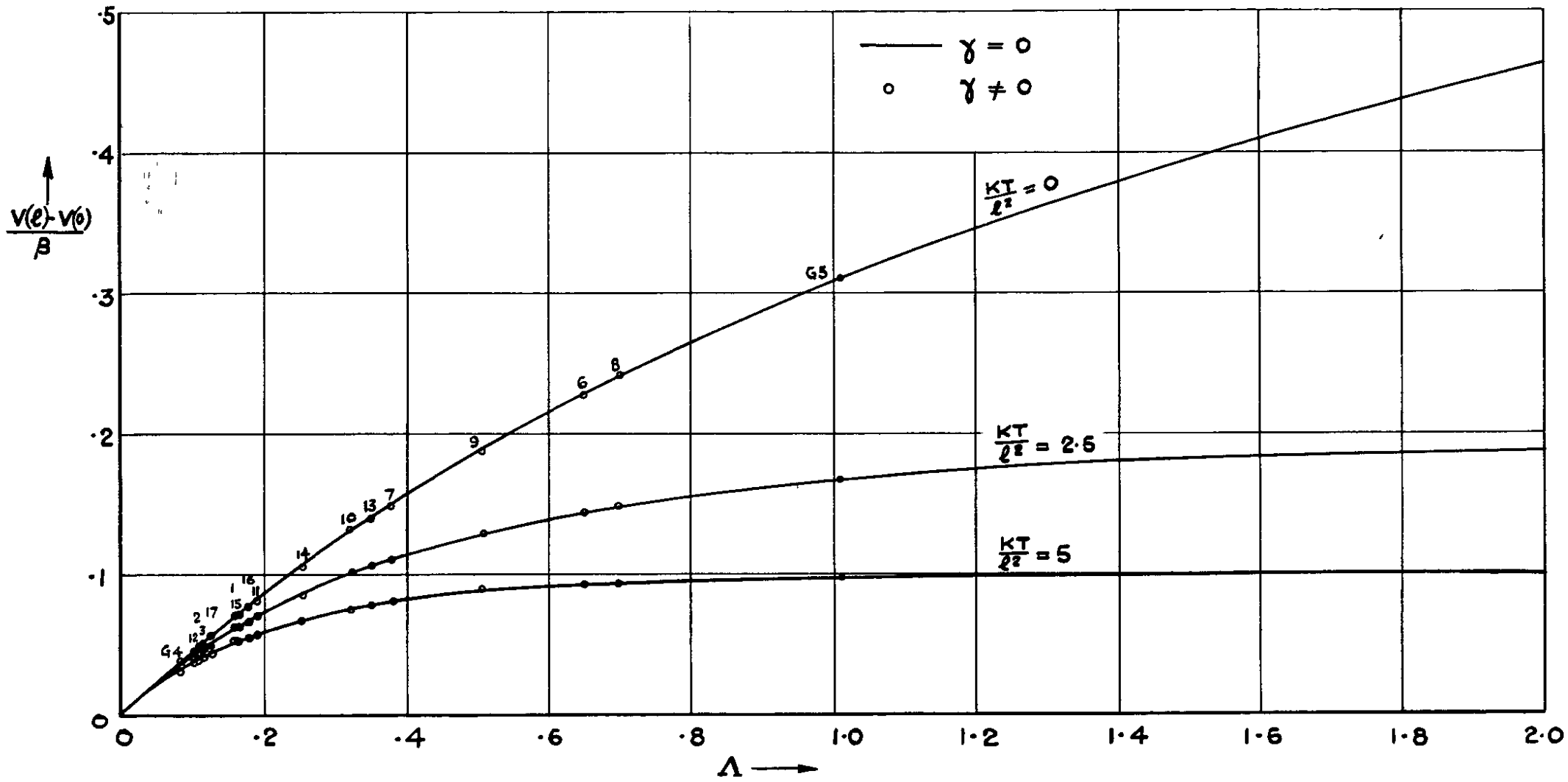

FIG.4. TEMPERATURE DIFFERENCES ACROSS SELECTED COMPOSITE SLABS

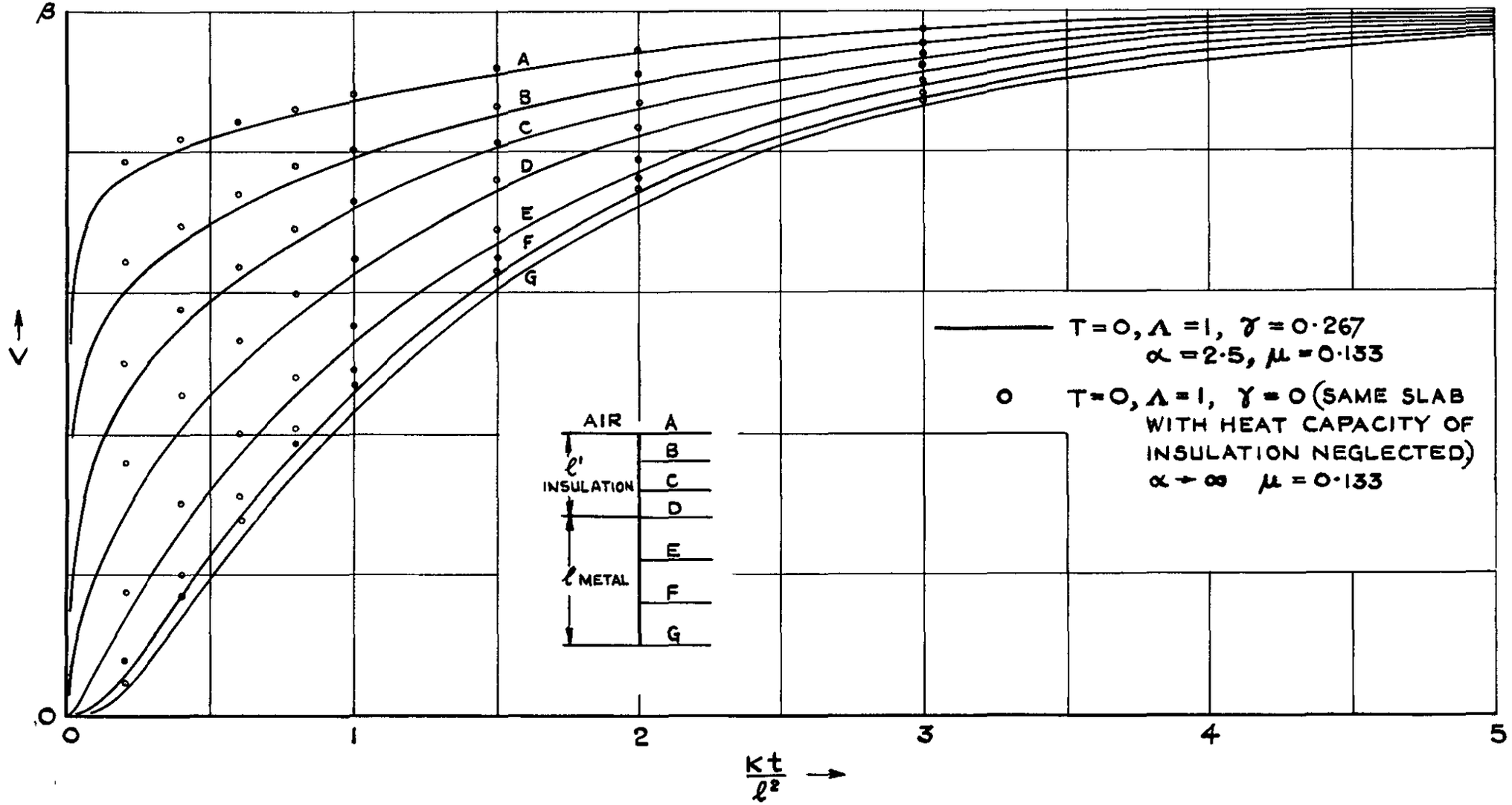

FIG.5. TEMPERATURE DISTRIBUTION IN A SAMPLE SLAB

C.P. No. 412
(20,499)
A.R.C. Technical Report

Published by
HER MAJESTY'S STATIONERY OFFICE

To be purchased from
York House, Kingsway, London w c 2
423 Oxford Street, London w 1
13A Castle Street, Edinburgh 2
109 St. Mary Street, Cardiff
39 King Street, Manchester 2
Tower Lane, Bristol 1
2 Edmund Street, Birmingham 3
80 Chichester Street, Belfast
or through any bookseller

Printed in Great Britain

S.O. Code No. 23-9011-12

C.P. No. 412